Research Square

Preprints are preliminary reports that have not undergone peer review.
They should not be considered conclusive, used to inform clinical practice,
or referenced by the media as validated information.

Synergistic regulation of defective meiotic DNA repair, premature tapetal degeneration, and hormone signaling underlies pollen abortion in Arundo donax

Ruihao Liu
Zhengzhou University
Yixin Huangfu
Zhengzhou University
Beibei Zhang
Zhengzhou University
Xinyu Tan
Zhengzhou University
Mengxin Huang
Zhengzhou University
Yong Liang
Zhengzhou University
Mingchen Yu
Zhengzhou University
Jialin Guo
Zhengzhou University
Zhengqing Xie
Zhengzhou University
Baoming Tian
Zhengzhou University
Gongyao Shi
Zhengzhou University
Fang Wei
fangwei@zzu.edu.cn
Zhengzhou University

Research Article

Keywords: Arundo donax, Meiosis, Tapetum, Pollen abortion, DNA repair, Transcriptome

Posted Date: September 23rd, 2026

DOI: https://doi.org/10.21203/rs.3.rs-10523110/v1

License: This work is licensed under a Creative Commons Attribution 4.0 International License.
Read Full License

Additional Declarations: No competing interests reported.

Synergistic regulation of defective meiotic DNA repair, premature tapetal degeneration, and hormone signaling underlies pollen abortion in *Arundo donax*

Ruihao Liu, Yixin Huangfu, Beibei Zhang, Xinyu Tan, Mengxin Huang, Yong Liang, Mingchen Yu, Jialin Guo, Zhengqing Xie, Baoming Tian, Gongyao Shi, Fang Wei*

Henan International Joint Laboratory of Crop Gene Resource and Improvements, School of Agriculture and Biomanufacturing, Zhengzhou University, Zhengzhou 450001, China.

Corresponding author

Fang Wei, fangwei@zzu.edu.cn

Abstract

Arundo donax L. is a highly promising bioenergy and forage crop; however, its seed set is frequently constrained by abnormalities in gametophyte development, and the mechanisms underlying pollen abortion remain unclear. In this study, we integrated morphological observation, scanning electron microscopy, paraffin sectioning, pollen germination assays, meiotic cytology, and transcriptome analysis to investigate the developmental and molecular basis of male gametophyte abortion. Mature anthers were shriveled and did not undergo normal dehiscence, leading to reduced pollen production and fertility. Cytological analysis revealed spindle defects during meiosis, leading to unequal chromosome segregation. Premature tapetal degeneration disrupted nutrient supply to developing microspores, resulting in pollen wall collapse and loss of viability at the tricellular stage. Transcriptome profiling showed that upregulated genes in the male gametophyte were enriched in membrane components, redox processes, and protein ubiquitination, accompanied by activation of ethylene (ET) and jasmonate signaling, indicating their potential involvement in the disruption of normal gametophyte development. Conversely, downregulated genes were primarily associated with microtubule binding, mitotic cell cycle progression, and DNA-binding activities. Kyoto Encyclopedia of Genes and Genomes (KEGG) analysis further indicated significant downregulation of genes involved in base excision repair, nucleotide excision repair, and homologous recombination, implying impaired DNA double-strand break repair during meiosis. These defects likely lead to abnormal chromosome behavior, defective microspore formation, and ultimately male gametophyte abortion. Collectively, these findings provide novel insights into the molecular basis of pollen abortion in *A. donax*.

Keywords *Arundo donax* · Meiosis · Tapetum · Pollen abortion · DNA repair · Transcriptome

Introduction

Arundo donax L., a perennial C3 herbaceous species belonging to the genus *Arundo* in the family Poaceae, has garnered growing global attention in the fields of ecological restoration, bioenergy development, and industrial applications, attributed to its robust rhizome system, remarkable environmental adaptability, and extensive utilization potential (Lino et al. 2023). *A. donax* requires relatively low inputs of water and nutrients, while exhibiting strong tolerance to cold, drought, and nutrient-deficient conditions. It grows vigorously along riverbanks, roadsides, sandy soils, and even on marginal lands that are unsuitable for conventional crop cultivation (Cristaldi et al. 2020). From an ecological standpoint, *A. donax* effectively mitigates soil erosion through its well-developed rhizome network; it also absorbs nitrates from aquatic environments, thereby reducing nutrient pollution and contributing to watershed protection. Furthermore, this species demonstrates a notable capacity for the uptake and remediation of heavy metal ions in contaminated soils (Zhang et al. 2021). Its leaves are rich in protein, rendering them a valuable forage resource, whereas its culms are abundant in lignocellulosic fibers and exhibit high efficiency in both biochemical and thermochemical conversion processes. These characteristics facilitate its wide-ranging applications in pulp production, fiberboard manufacturing, and bioethanol processing. Additionally, by-products generated during the processing process can be further exploited for the extraction of antioxidants, realizing comprehensive and efficient resource utilization (Corno et al. 2014). In recent years, driven by the global demand for renewable energy, *A. donax* has been increasingly recognized as a highly promising bioenergy crop, owing to its exceptional biomass yield and prominent environmental resilience.

A. donax exhibits extensive taxonomic diversity and is typically characterized as a polyploid complex with broad variation in chromosome numbers (2n = 36, 48, 54, 72, 90). Severe abnormalities in both male and female gametophyte development are common, and flowering plants frequently fail to produce viable seeds capable of normal germination (Sánchez et al. 2021). Consequently, current propagation relies predominantly on vegetative methods such as clump division and stem cuttings, which greatly restricts the feasibility of genetic improvement through hybrid breeding (Roberto Pilu 2012). As the male reproductive organ of angiosperms, the stamen plays a decisive role in determining pollen fertility and the plant's overall seed-setting capacity. Pollen development is a

highly ordered and intricate biological process that encompasses several key stages, including anther morphogenesis, meiotic division of pollen mother cells, microspore release, male gametophyte formation, and anther dehiscence (Gómez et al. 2015). During these stages, the tapetum, the innermost secretory cell layer of the anther wall-supports microspore development by supplying nutritional resources and structural precursors through a tightly regulated program of spatiotemporal differentiation and programmed cell death; its proper function is essential for pollen wall formation and the maintenance of pollen viability (Wei and Ma 2023). The cytoskeleton, particularly microtubules and actin filaments, undergoes dynamic reorganization throughout meiosis, playing crucial roles in ensuring accurate chromosome segregation, determining the division plane, and facilitating cell plate formation (Tidy et al. 2022). Previous studies have shown that cytoskeletal abnormalities often arise as early as the pollen mother cell stage in many aborted microspores (Wang et al. 2025). For example, in photoperiod- and thermo-sensitive genic male sterile rice lines, microtubules in microsporocytes are reduced in number and loosely organized during the late leptotene-zygotene transition, and they exhibit abnormal thickening during meiosis. Such alterations can serve as early indicators of pollen abortion (Zhou et al. 2024).

The pollen abortion observed in *A. donax* involves a complex interplay of genetic and cytological factors. Existing studies indicate that the mechanisms underlying sterility vary considerably across geographic regions. In the Mediterranean region, variation in ploidy levels among *A. donax* populations leads to differences in pollen stainability; however, pollen germination rates remain uniformly low. These abnormalities are accompanied by extensive pollen wall collapse and anther cavitation, with asymmetric chromosome segregation and lagging chromosomes during meiosis considered the primary causal factors. Nonetheless, the limited seed set observed under interspecific mixed planting conditions suggests that self-incompatibility may also contribute to sterility (Hardion et al. 2015). In the Columbia floodplain of the United States, *A. donax* exhibits extremely low microspore production, premature degeneration of the tapetum and middle layer, and insufficient structural support for gametophyte development. Concurrently, the development of the female megaspore is arrested, ultimately preventing the formation of mature female gametophytes (Balogh et al. 2012). In the Nagpur region of India, similar abnormalities have been reported, including a reduced number of sporogenous cells, early degradation of the middle layer, dysfunctional tapetal cells, and inadequate starch accumulation in pollen grains (Nikhade and Makde 2014). In southeastern Australia, *A. donax* populations characterized by high genetic variability and heterogeneous ploidy levels exhibit malformed anthers devoid of pollen (Haddadchi et al. 2013). Collectively, these studies demonstrate that fertility defects in *A. donax* arise from a complex integration of genetic background, meiotic chromosome behavior, cytological structural dynamics, and physiological metabolism. However, the cellular and molecular mechanisms underlying its sterility remain incompletely understood and warrant further in-depth investigation.

Therefore, in this study, *A. donax* was used as the research material, and its stamen developmental process was systematically investigated through cytological observations, physiological and biochemical analyses, and molecular approaches. Particular emphasis was placed on key developmental events, including tapetum differentiation and degeneration dynamics, meiotic chromosome behavior, and pollen wall formation. The aim of this study was to elucidate the cytological and molecular mechanisms underlying its pollen abortion in *A. donax*, thereby providing a scientific basis for germplasm conservation, genetic improvement, and its efficient utilization.

Materials and methods

Plant materials

The plant materials of *A. donax* used in this experiment were sourced from the cultivation base of the School of Agriculture and Biomanufacturing, Zhengzhou University, and all plants were grown under natural environmental conditions.

Observation of the flowering process

During the flowering period of *A. donax*, flowering individuals were regularly monitored to characterize their basic flowering traits. The recorded floral morphological parameters included flowering duration, number of florets per spikelet, spikelet pedicel length, spikelet length, mature anther length, pistil length, palea length, and floral organ coloration.

Ultrastructural observation of anthers and pollen grains

For each preparation, 10-15 mature, non-dehiscent anthers were placed on a glass slide, and a drop of distilled water was added. The anthers were transversely sectioned using a razor blade, and pollen grains were gently released with a dissecting needle. Excess anther wall debris was removed using fine forceps. Pollen samples were stained separately with I_2-KI solution and Alexander's stain (Peterson et al. 2010) After applying a coverslip and allowing staining to proceed for 10 min, the slides were examined and imaged under a light microscope. For quantitative assessment, 10 slides were randomly selected per treatment, and three fields of view per slide were analyzed to estimate pollen viability (Alexander's stain) and stainability (I_2-KI).

Determination of pollen germination ability

Pollen grains were collected from a large number of mature, unpollinated florets. For each germination assay, a 50 μL aliquot of liquid germination medium (containing 5% sucrose, 0.04% boric acid, and 0.03% calcium chloride) was placed at the center of a glass slide. A small amount of pollen was transferred into the droplet using a dry fine brush and evenly dispersed by gentle tapping. A square Petri dish was prepared with a layer of moistened filter paper to maintain high humidity. The slide was elevated above the filter paper using a support (e.g., a glass rod or plastic rack) to prevent excess moisture from entering the medium droplet. The Petri dish was then covered and incubated at 25℃ for 1, 2, 3, 4, 5, and 6 h. Five replicate slides were prepared for each incubation period. For each replicate, five fields of view were randomly selected and examined under a light microscope. Pollen germination was defined as the emergence of a pollen tube with a length exceeding twice the diameter of the pollen grain (Chen et al. 2025).

Observations of meiosis in pollen mother cells

Fresh anthers at different developmental stages were stripped and immersed in a drop of modified magenta solution placed on a slide. The anthers were gently crushed using a dissecting needle to release pollen mother cells from the pollen sacs. Impurities were carefully removed using forceps, coverslips were placed over the samples, and the slides were observed under a microscope for stage identification. If microspore mother cells were identified to be in the pre-meiotic stage, the remaining anthers were digested in 2% enzyme solution at 37℃ for 14 hours, followed by hypotonic treatment in distilled water at room temperature for 2 hours. Preheated 60% glacial acetic acid (at 40℃) was prepared in advance. A drop of distilled water (20 μL) was placed on the slides, and 2-3 hypotonic anthers were crushed gently using a dissecting needle. Approximately 20 μL of preheated 60% glacial acetic acid was then added to the slide, and the liquid was spread evenly across the slide surface using a dissecting needle. The slide was placed on a baking machine set at 40℃ until the liquid adopted a stellate appearance. Impurities on the slide were rinsed off with Carnoy's fixative, followed by drying on the baking machine. Finally, a drop of PI staining solution was applied to the slide, a coverslip was placed, and the samples were observed and photographed under a fluorescence microscope.

Microtubule immunofluorescence

For the detection of β-tubulin, procedures from a previous study were adopted (Yang et al. 2017), with few modifications Fresh anthers were collected and immediately fixed in 4% paraformaldehyde. Pollen mother cells were first sealed with 5% bovine serum albumin for 1 h. PMC were incubated with a monoclonal antibody against β-microtubulin (Sigma-Aldrich, St. Louis, MO, USA) at a ratio of 1:100 in a wet room at 4°C for 12 h. PMC were then incubated with a fluorescein isothiocyanate (FITC)-coupled anti-mouse antibody (SigmaAldrich St. Louis, MO, USA) at a ratio of 1:100 in a dark room at 37°C for 2 h. Then, after rinsing three times in PBS, the cell

solution was dropped on a clean slide and then stained with 40 g/mL PI. The prepared glass slides were observed and imaged with a Carl Zeiss confocal laser scanning microscope (LSM 880, Carl Zeiss AG, Oberkochen, Germany).

Observations on the development of the male gametophyte

Collect florets of different developmental periods, after one anther was identified as being in the gametophyte development stage, the other two anthers were taken and stained with 4′,6′-diamidino-2-phenylindole (DAPI, Sigma-Aldrich, St. Louis, MO, USA) fluorescent stain (Lou et al. 2018), avoiding light for more than 2 h, covered Alexander with a coverslip, and then photographed in fluorescence and white field under the fluorescence microscope, to observe the developmental process of the male gametophyte, and randomly selected 10 slides, with 3 fields of view on each slide, and counted the proportion of normal and abnormal male gametophytes and the types of abnormalities. The proportion of normal and abnormal male gametophytes and the type of abnormality were counted.

Observations on the development of the downy layer

Anthers of the identified stages were first fixed in formalin-ethanol (FAA) under vacuum for 1 h, then dehydrated in a graded ethanol series and paraffin-embedded (Leica, Wetzlar, Germany) after transparency in a transparent medium (xylene). Sections (8 μm) were obtained with a Leica Reichert Supernova microtome (Leica, Wetzlar, Germany), placed on glass slides, and stained with Safranin O-Fast Green staining (Solarbio, Beijing, China) according to the manufacturer's specifications. Sections were examined with a fluorescence microscope (Olympus BX43, Tokyo, Honshu, Japan) and images were captured with a CCDDP73 camera (Olympus, Tokyo, Japan) connected to CellSens standard software.

Functional Annotation of Differentially Expressed Genes (DEGs)

The inflorescences and leaves were collected from each growth period, and the stamens and pistils were separated, RNA was extracted, and the RNA samples that met the sequencing conditions were divided into 2 copies, 1 copy was sent to Meiji Biomedical Technology Co. Ltd. for the construction of cDNA libraries and sequencing of transcriptomes, and 1 copy was stored in the refrigerator at -80°C for subsequent RT-qPCR validation. The sequencing data were subjected to quality control and re-assembly, and the transcriptome expression level was quantitatively analysed using the software RSEM (Li and Dewey 2011) and the FPKM value (Fragments Per Kilobase of exon model per Million mapped fragments) was used as a measure of the gene expression level. After obtaining the Read Counts of the genes, DESeq2 was used to analyse the differential expression of the genes among multiple samples by calculating the p-value using the Wald test， and the p-value was corrected to obtain the p-value by the BH Multiple Test Correction Method. p-value was obtained when the Fold Change (FC) was ≥ 2 and p-value ≤ 0.05. the gene was considered to be differentially expressed, and thus DEGs were identified.

Results

Floral Morphology and Pollen Abortion in *A. donax*

Abnormal inflorescences of *A. donax* were selected for observation in this study. The results showed that the panicles were relatively small, with few branches, and that the apical spikelets failed to develop, whereas the remaining spikelets were morphologically comparable in size to those of normal plants (Fig. 1a). At this stage, the majority of anthers within the florets appeared shriveled and adherent, exhibiting a necrotic coloration (Fig. 1b). Both stamens and pistils displayed a high frequency of morphological abnormalities, primarily characterized by reduced anther size, surface shrinkage, and asymmetrical shapes. In addition, considerable morphological variation was observed among abnormal stamens, indicating that sterility occurs along a continuum of phenotypic variation rather than as a single discrete type (Fig. 1c).

To further investigate the structural characteristics of sterile anthers, the ultrastructure of the anthers and pollen grains was examined. Scanning electron microscopy revealed that the anthers possessed distinct stomium

grooves and contained four pollen sacs (Fig. 1d), with longitudinal striations observed on the surface (Fig. 1e). Pollen grain imaging revealed extensive abnormalities, including shrunken and flattened grains with marked size heterogeneity (Fig. 1f). The germination apertures were invaginated, and the exine surrounding the apertures was thickened (Fig. 1g).

Pollen viability and fertility were subsequently assessed. Using Alexander staining, only a small proportion of pollen grains stained purple-red, whereas most grains remained unstained, weakly stained, or unevenly stained, indicating low pollen viability in *A. donax* (Fig. 1h). I_2-KI staining further revealed three types of abortive pollen: typical abortion, spherical abortion, and staining abortion (Fig. 1i). Quantitative analysis showed that the proportions of typical abortion, spherical abortion, and staining abortion were 38.53%, 27.65%, and 24.38%, respectively, whereas normal pollen grains accounted for only 8.12% (Fig. 1j). In addition, fused pollen grains were observed, along with significant variation in pollen size. Some pollen grains were stained dark brown but were markedly larger than normal pollen grains.

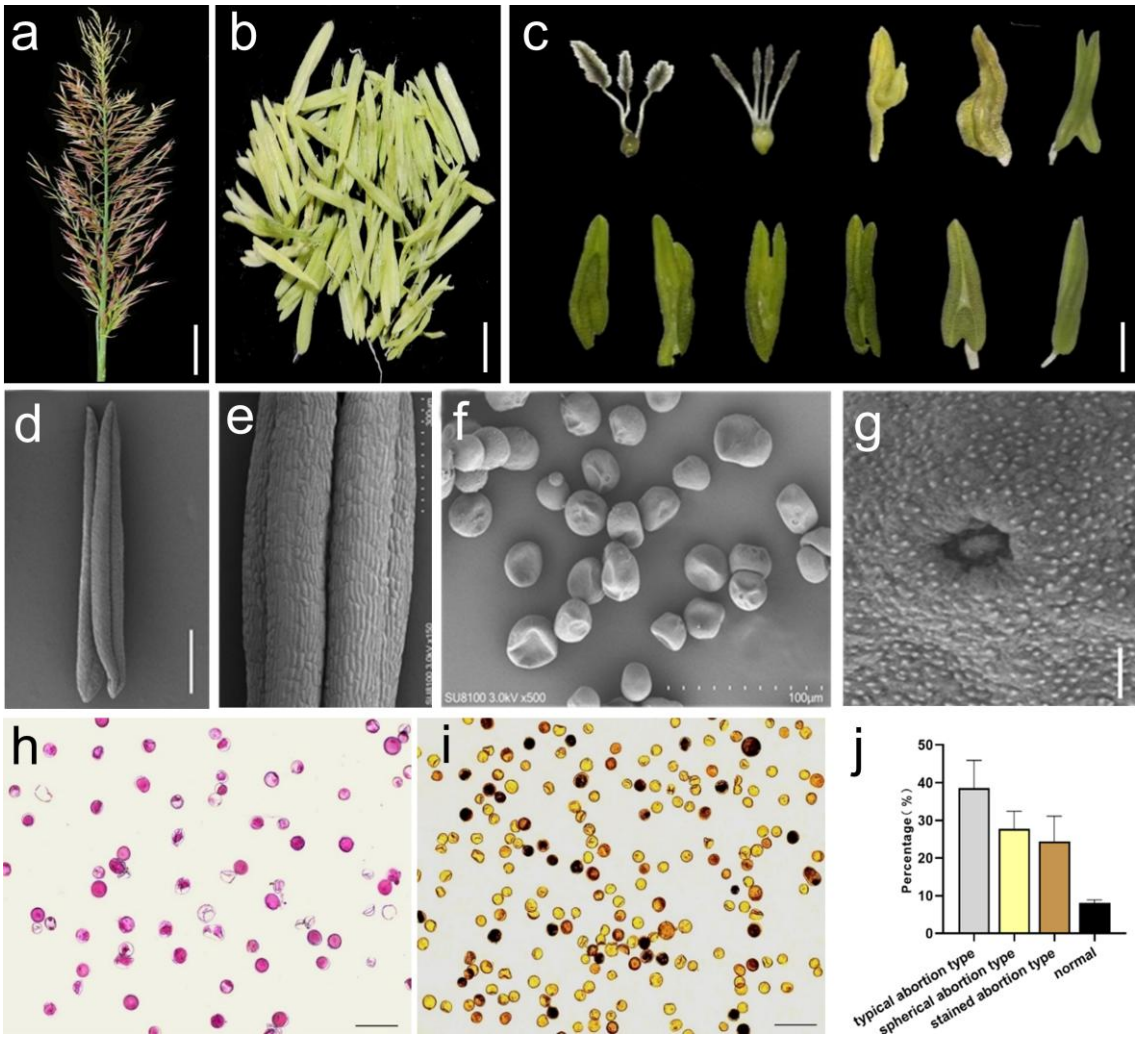

Fig. 1 Floral organ morphology and pollen grain observation of abortive *A. donax*. **a** Abnormal inflorescence of super giant reed, scale bar = 3 cm. **b** Shrivelled anthers of super giant reed, scale bar = 1 mm. **c** Aberrant morphology of pistils and stamens, scale bar = 1 mm. **d** Ultrastructural observation of anthers, scale bar = 0.25 mm. **e** Ultrastructural observation of anthers. **f** Ultrastructural observation of pollen grains. **g** Abnormal germinal aperture, scale bar = 2 μm. **h** Alexander staining of super giant reed pollen grains. **i** I_2-KI staining of super giant reed pollen grains, scale bar = 100 μm. **j** Statistical analysis of the proportion of different abortive pollen types and normal pollen grains, n = 10

Premature Degeneration of the Tapetum During Anther Wall Development in *A. donax*

Previous studies have demonstrated that abnormal development of the tapetum can significantly affect pollen fertility (Moon et al. 2020). In this study, paraffin sectioning was performed to examine anther development in *A. donax* during meiosis. The results showed that, at the early meiotic stage (Fig. 2a), tapetal cells were polygonal, irregularly arranged, and incompletely connected. They were relatively distant from the middle layer cells, with some partially detaching from the anther wall and shifting inward toward the locule. Transverse intercellular spaces were enlarged, and the tapetum underwent premature and abnormal degeneration. Meanwhile, pollen mother cells within the locule were observed at multiple meiotic stages simultaneously, with reduced numbers and evident shrinkage.

At the subsequent stage (Fig. 2b), tapetal cells further degraded and became completely detached from the anther wall. A few abnormally degraded cells even intruded into the anther locule. When development reached the uninucleate stage (Fig. 2c), the tapetum had completely degenerated, leaving only the epidermis and two layers of endothecium in the anther wall. The endothecium gradually exhibited longitudinal thickening. During the binucleate and trinucleate stages (Fig. 2d), microspores within the pollen sacs appeared shrunken and deformed, with uneven distribution of cellular contents, indicating severe pollen abortion.

Abnormal morphological features were also observed in paraffin sections across different stages of pollen development. Pollen mother cells were spherical and loosely arranged (Fig. 2e). Microspores had formed, but their cytoplasm was sparse, and some exhibited incomplete development. The anther wall layers became relatively thinner, and tapetal cells showed signs of collapse (Fig. 2f). The number of microspores in the locule decreased, and their morphology became irregular, with some showing shrinkage or distortion, reflecting asynchronous development. Meanwhile, the surrounding anther wall layers continued to thin (Fig. 2g). At later stages, the number of pollen grains was further reduced, with pronounced morphological variation, including malformed or degenerated grains. Some pollen grains exhibited intensified staining or appeared fragmented, suggesting ongoing degeneration. The anther wall layers also became markedly thinner and structurally loosened (Fig. 2h). These results indicate that abnormalities in *A. donax* anther development, including shrinkage and structural defects, are initiated at early developmental stages.

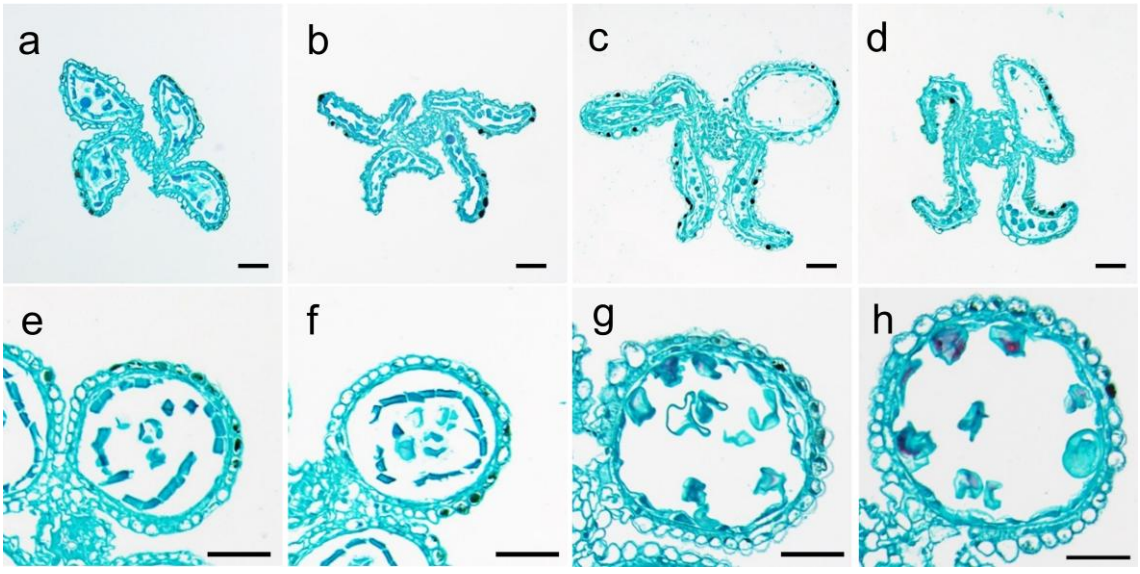

Fig. 2 Paraffin sections of super giant reed anthers. **a-d** Aberrant morphological features of anthers at different developmental stages revealed by paraffin sectioning. **e** Paraffin section of an anther at early meiosis. **f** Paraffin section of an anther at late meiosis. **g** Paraffin section of an anther at the uninucleate stage. **h** Paraffin section of an anther at the binucleate and trinucleate stages. Scale bars = 50 μm

Low Pollen Germination Rate in *A. donax*

To investigate pollen germination and pollen tube growth in *A. donax*, collected pistils were stained with aniline blue and observed under a fluorescence microscope. The results showed that (Fig. 3a-d) very few pollen grains were deposited on the stigma, with only a small number detected on a limited number of stigmas, and no pollen tube elongation was observed. Furthermore, no fluorescence signals were detected in the style or ovary of any pistils examined, indicating the absence of successful pollen tube penetration and growth.

Subsequently, in vitro pollen germination assays were conducted. The results revealed that, in some pollen grains, the cytoplasm accumulated near the germination aperture, forming a vesicle-like structure, after which growth ceased without further elongation. This was often accompanied by leakage of cellular contents. In addition, some pollen tubes were extremely short, whereas others exhibited twisting and deformation. An abnormal phenomenon was also observed in which two pollen tubes emerged from a single germination aperture (Fig. 3e). Analysis of pollen germination showed that pollen tube elongation occurred during germination and that the germination rate increased over time. The most rapid increase was observed within the first hour. The germination rate reached its maximum at 2 h of incubation, but was only 1.66%. After 2 h, the germination rate remained similar to that at the second hour and gradually stabilized, showing little further change over time. Overall, the pollen grains failed to germinate normally (Fig. 3f).

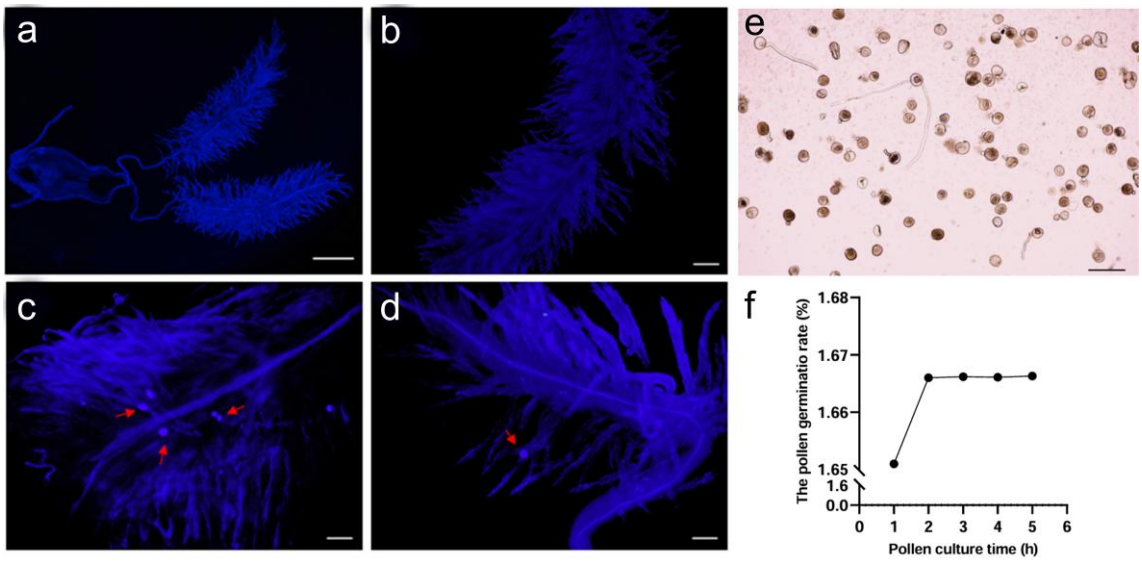

Fig. 3 Observation of pollen tube growth via in situ pollen germination. **a** No pollen grains or pollen tube growth observed on the entire pistil, scale bar = 200 μm. **b** No pollen grains or pollen tube growth observed on a single stigma, scale bar = 100 μm. **c-d** A small number of pollen grains present on the stigma but no pollen tubes visible, scale bars = 50 μm. **e** In vitro germination of super giant reed pollen grains. **f** Pollen germination rate of super giant reed

Meiotic Abnormalities and Disrupted Chromosome Behavior Leading to Pollen Abortion in *A. donax*

Previous studies have demonstrated that the development of pollen mother cells (PMCs) and male gametophytes is critically dependent on proper meiotic chromosome behavior. In this study, the development of PMCs and male gametophytes in *A. donax* was systematically investigated. The results revealed pronounced abnormalities in chromosome segregation and cytokinesis during meiosis I. Lagging chromosomes were observed at metaphase I (Fig. 4a), while chromosome bridges were detected at anaphase I (Fig. 4b). Unequal division of dyads was evident at telophase I (Fig. 4c-d), characterized by asynchronous chromosome segregation and uneven cytoplasmic partitioning (Fig. 4e). Morphologically abnormal tetrads were observed following meiosis I (Fig. 4f), indicating defects in chromosome segregation, spindle organization, and cytokinesis. Abnormal microspores

exhibited disorganized exine structures and collapsed cytoplasmic contents (Fig. 4g1, g2). Some microspores retained intact exine outlines but lacked normal cellular architecture (Fig. 4h1, h2), whereas others showed severe collapse accompanied by cytoplasmic fragmentation (Fig. 4i1, i2). These observations suggest that both exine deposition and intracellular structural integrity were disrupted during microspore development.

Immunofluorescence analysis of tubulin further revealed that univalent chromosomes in late meiosis migrated randomly toward both poles, accompanied by weak microtubule signals and the absence of a properly formed spindle apparatus (Fig. 4j). Similar abnormalities were observed at metaphase I (Fig. 4k). In addition, reduced spindle tension and lagging chromosomes were detected during anaphase I (Fig. 4l), and asynchronous division persisted through telophase II (Fig. 4m). Collectively, these findings indicate that PMCs of *A. donax* exhibit aberrant chromosome behavior, defective cytokinesis, impaired microspore formation, and disrupted spindle organization during meiosis and male gametophyte development, which likely contribute to pollen abortion.

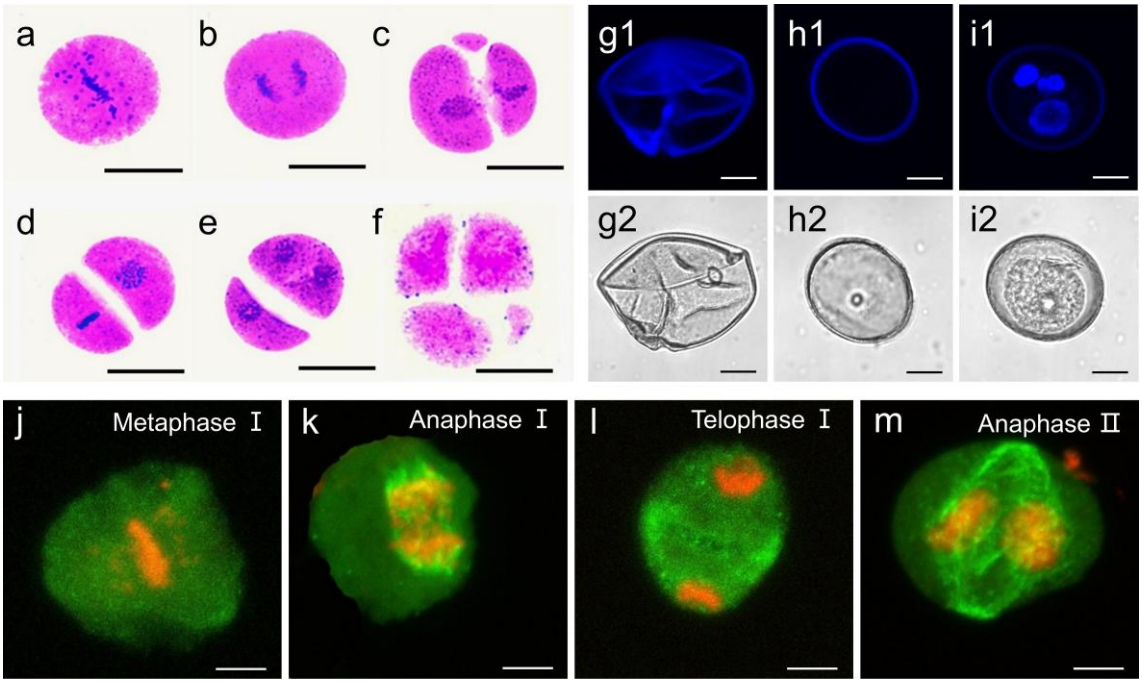

Fig. 4 Meiotic abnormalities in pollen mother cells and immunofluorescence observation of tubulin in super giant reed. **a** Lagging chromosomes at metaphase I. **b** Formation of a chromatin bridge at anaphase I. **c** Unequal cytokinesis at telophase I. **d** Asynchronous chromosome segregation at metaphase II. **e** Asynchronous chromosome segregation and unequal cytokinesis at anaphase II. **f** Unequal segregation of cytoplasm and chromosomes at telophase II resulting in aberrant tetrads. Scale bars = 20 μm. (**g1-i1**, **g2-i2**) Developmental progression of abnormal microspores. Scale bars = 10 μm. **j** Aberration at metaphase I. **k** Aberration at anaphase I. **l** Aberration at telophase I. **m** Aberration at anaphase II. Scale bars = 5 μm

Identification of Upregulated DEGs Associated with Pollen Abortion in *A. donax*

To investigate the characteristics of pollen abortion in *A. donax*, we analyzed genes that were upregulated in stamens relative to pistils. Venn diagram analysis revealed that 21,961 genes were commonly upregulated in both stamens and pistils, while 22,494 genes were shared between stamens and leaves, with 12,440 genes consistently upregulated in stamens relative to both leaves and pistils (Fig. 5a). To further elucidate the regulatory mechanisms underlying stamen development, Gene Ontology (GO) enrichment analysis was conducted on the 21,961 upregulated genes (Fig. 5b). The results indicated that these genes were significantly enriched in GO terms associated with membrane related components and processes, including protein ubiquitination. Significant enrichment was also observed in terms related to redox processes and corresponding enzymatic activities, as well

as intrinsic and integral components of membranes (Fig. 5c). Subsequent analysis of genes involved in protein ubiquitination revealed a general trend of upregulation in stamens compared with pistils (Fig. 5d). Collectively, these findings suggest that pollen abortion in *A. donax* may be associated with substantial alterations in membrane protein expression, enhanced redox-metabolism or reactive oxygen species (ROS) imbalance, and activation or dysregulation of the ubiquitin-mediated protein degradation pathway, thereby potentially contributing to pollen abortion.

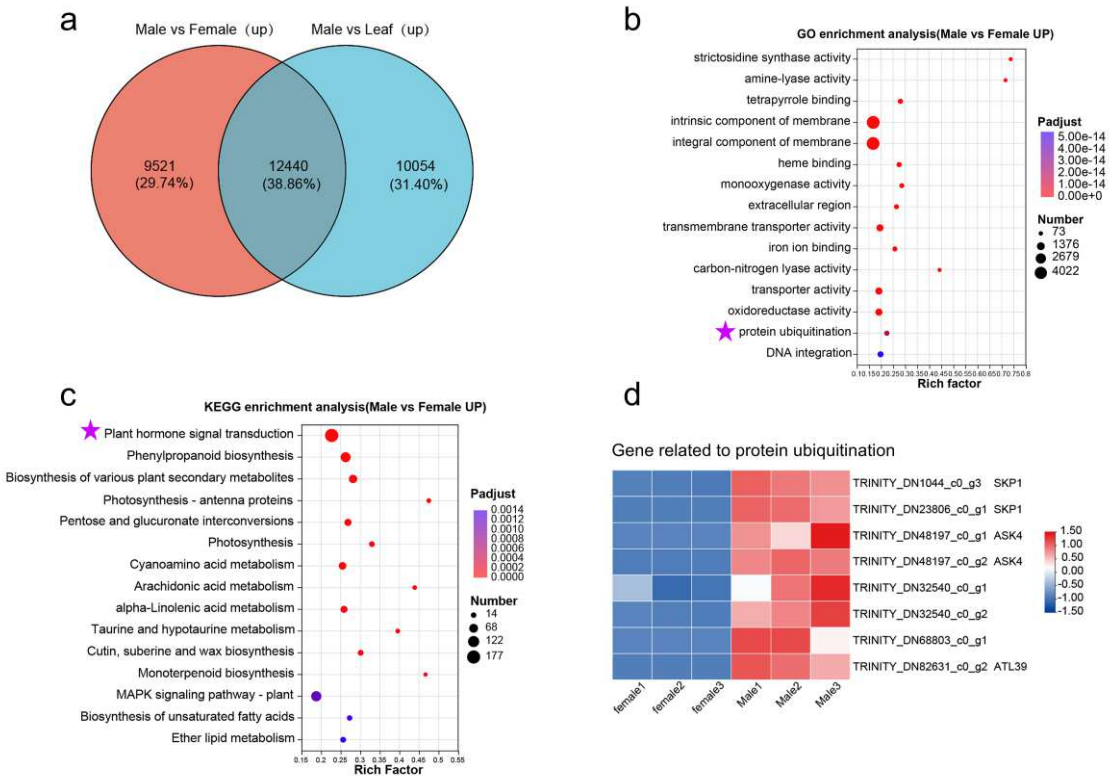

Fig. 5 Functional classification of upregulated gene set preferentially expressed during male gamete development. **a** Venn diagram showing the overlap of upregulated genes between Male vs. Leaf and Male vs. Female. **b** GO enrichment analysis of preferentially expressed genes in Male. **c** KEGG enrichment analysis of preferentially expressed genes in Male. **d** Protein ubiquitination related genes expression pattern in Male vs. Female

To investigate the regulatory mechanisms underlying pollen abortion in *A. donax*, KEGG enrichment analysis was conducted on the 21,961 upregulated DEGs. This analysis aimed to elucidate the involvement of these genes in specific biological processes and metabolic pathways potentially associated with stamen sterility. The results indicated that the upregulated DEGs were predominantly enriched in pathways related to plant hormone signal transduction, the plant Mitogen-Activated Protein Kinase (MAPK) signaling pathway, and the biosynthesis of cutin, suberin, and waxes (Fig. 5c).

To further dissect the hormonal regulation underlying pollen abortion, we focused on the KEGG enrichment results for plant hormone signal transduction pathways. Notably, this pathway was significantly enriched. We subsequently characterized the core components of the ET signaling pathway (Fig. 6a) and the jasmonic acid (JA) signaling pathway (Fig. 6b), together with their transcriptomic expression profiles in stamens. Within the ET signaling pathway, the hormone receptors Ethylene Receptor (*ETR*) were significantly upregulated in stamens, accompanied by increased expression of the downstream regulator Constitutive Triple Response 1 (*CTR1*). This, in turn, indirectly inhibited Stress-Induced Mitogen-Activated Protein Kinase Kinase (*SIMKK*) within the MAPK cascade. The phosphorylation status of *SIMKK* was associated with the activation of Mitogen-Activated Protein

Kinase 6 (*MPK6*), thereby enhancing intracellular ET signal transduction. Concurrently, the key cytoplasmic nuclear signaling component Ethylene Insensitive 2 (*EIN2*) and the central transcription factor Ethylene Insensitive 3 (*EIN3*) were significantly upregulated in stamens. Furthermore, the ubiquitin-related factors EIN3-Binding F-box 1/2 (*EBF1/EBF2*), which mediate the ubiquitination and degradation of *EIN3*, were also significantly upregulated, followed by the activation of downstream transcription factors Ethylene Response Factor 1/2 (*ERF1/ERF2*). Similarly, the JA signaling pathway was upregulated in stamens. The increased expression of Jasmonic Acid Resistant 1 (*JAR1*), which encodes a rate-limiting enzyme in JA-Ile biosynthesis, likely altered the accumulation dynamics of the bioactive JA conjugate, thereby activating the JA receptor Coronatine Insensitive 1 (*COI1*). This activation subsequently promoted the ubiquitination of Jasmonate ZIM-domain (*JAZ*) repressor proteins, whose corresponding genes were also significantly upregulated in stamens leading to JAZ degradation and the release of the transcription factor Myelocytomatosis 2 (*MYC2*).

Collectively, these findings indicate that both the ET and JA signaling pathways are enhanced in the stamens of *A. donax*. The activation of these two hormonal signaling cascades may coordinate key cellular processes involved in stamen development, including signal transduction, cell fate specification, programmed cell death, and anther wall function, thereby synergistically contributing to pollen abortion in *A. donax*.

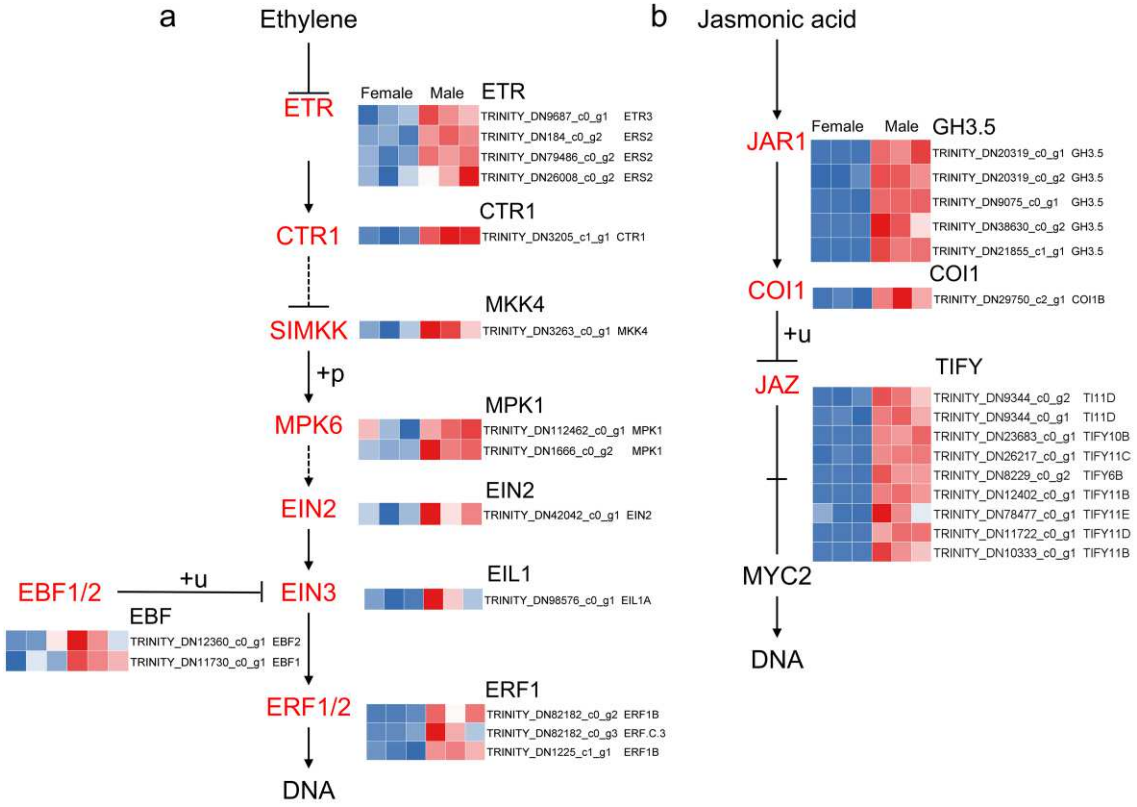

Fig. 6 Expression patterns of DEGs enriched in upregulated hormone signal transduction pathway. **a** ET signal transduction pathway. **b** JA signal transduction pathway. The heat maps indicated relative expression levels of genes. ETR, Ethylene Receptor; CTR1, Constitutive Triple Response 1; SIMKK, SIMK Kinase; MKK4, Mitogen-Activated Protein Kinase Kinase 4; MPK6, Mitogen-Activated Protein Kinase 6; MPK1, Mitogen-Activated Protein Kinase 1; EIN2, Ethylene Insensitive 2; EBF1/2, EIN3-Binding F-box 1/2; EIN3, Ethylene Insensitive 3; EIL1, Ethylene Insensitive 3-Like 1; ERF1, Ethylene Response Factor 1; ERF1/2, Ethylene Response Factor 1/2; MYC2, Myelocytomatosis 2; ETR3, Ethylene Receptor 3; JAR1, Jasmonic Acid Resistant 1; GH3.5, Gretchen Hagen 3.5; COI1, Coronatine Insensitive 1; JAZ, Jasmonate ZIM-domain; TIFY, TIFY domain protein. +p,

phosphorylation; +u, ubiquitination

Identification of downregulated DEGs Associated with Pollen Abortion in *A. donax*

To further investigate the characteristics of pollen abortion in *A. donax*, we analyzed genes that were downregulated in stamens relative to pistils during development. Venn diagram analysis revealed that 11,368 genes were downregulated in stamens compared with pistils, whereas 19,550 genes were downregulated in stamens compared with leaves, with 3,002 genes commonly downregulated in stamens relative to both leaves and pistils (Fig. 7a). To further elucidate the regulatory mechanisms underlying stamen development, GO enrichment analysis was conducted on the 11,368 downregulated DEGs (Fig. 7b). The results indicated that these downregulated genes were significantly enriched in GO terms associated with cytoskeletal organization, microtubule dynamics, and cell cycle and division processes, including microtubule binding and regulation of the mitotic cell cycle. Significant enrichment was also observed in GO terms related to DNA binding (Fig. 7c). Subsequent analysis of the expression patterns of genes involved in the mitotic cell cycle and microtubule binding revealed an overall trend of downregulation in stamens relative to pistils (Fig. 7d). Collectively, these findings suggest that stamens may undergo cell proliferation arrest or premature terminal differentiation, exhibiting markedly reduced mitotic activity and DNA-binding capacity, thereby contributing to pollen abortion in *A. donax*.

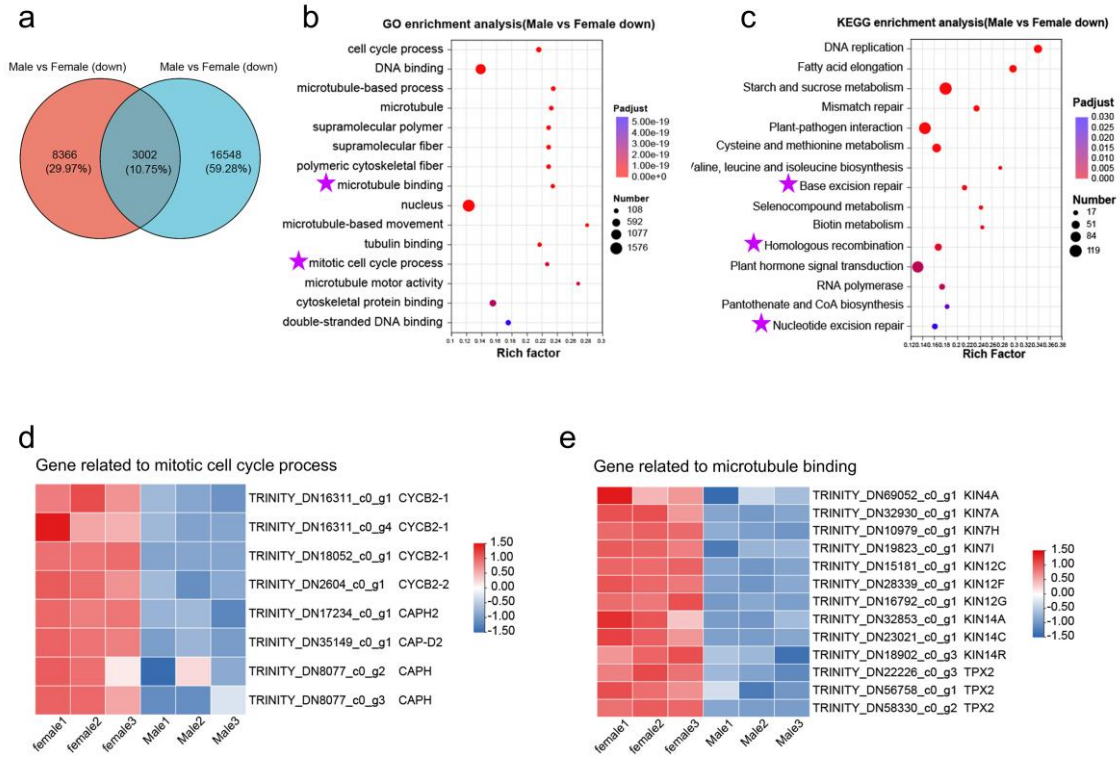

Fig. 7 Functional classification of downregulated gene set preferentially expressed during male gamete development. **a** Venn diagram showing the overlap of downregulated genes between Male vs. Leaf and Male vs. Female. **b** GO enrichment analysis of preferentially expressed genes in Male. **c** KEGG enrichment analysis of preferentially expressed genes in Male. **d** Mitotic cell cycle process related genes expression pattern in Male vs. Female. **e** Microtubule binding related genes expression pattern in Male vs. Female

Subsequently, KEGG enrichment analysis was performed on the 11,368 downregulated DEGs to investigate their involvement in biological processes and metabolic pathways associated with meiosis, thereby providing insights into the mechanisms underlying pollen abortion in *A. donax*. The results indicated that these genes were primarily enriched in pathways related to base excision repair (BER), nucleotide excision repair (NER), and homologous recombination (HR) (Fig. 7c).

To further elucidate the regulatory mechanisms of pollen abortion in relation to DNA repair, we analyzed the core components of the BER, NER, and HR pathways and examined their transcriptomic expression profiles. In the NER pathway (Fig. 8a), genes responsible for DNA damage recognition, including Xeroderma Pigmentosum complementation E (*XPE*), Xeroderma Pigmentosum complementation C (*XPC*), and the Cullin 4-Cockayne Syndrome A (*Cul4-CSA*) complex, were significantly downregulated in stamens, thereby impairing the early detection of DNA lesions. Genes involved in DNA unwinding, such as eroderma Pigmentosum complementation G (*XPG*) and members of the Replication Protein A (*RPA*) protein family, were also significantly downregulated, potentially affecting subsequent single-strand incision. During the incision, excision, and DNA synthesis stages, key factors, including Proliferating Cell Nuclear Antigen (*PCNA*) and the Replication Factor C (*RFC*) complex, were markedly downregulated, which may hinder new strand synthesis. Finally, the downregulation of DNA ligase I (*Lig I*) likely impaired the ligation of the DNA backbone.

Similarly, BER pathway (Fig. 8b) exhibited an overall downregulation trend in stamens. Initial lesion recognition by monofunctional glycosylases, such as 3-Methyladenine DNA Glycosylase I (*Tag*) and Uracil-DNA Glycosylase (*UNG*), was reduced, thereby affecting the identification and removal of damaged bases. The Apyrimidinic Endonuclease 2 (*APE2*) was also significantly downregulated, potentially compromising strand cleavage at abasic sites. During gap filling and strand displacement, the coordinated downregulation of factors, including DNA polymerase δ (*pol δ*), PCNA, and Flap Endonuclease 1 (*FEN1*), likely impaired base replacement and consequently affected DNA Ligase 1 (*Lig1*) -mediated ligation.

In the HR pathway (Fig. 8c), early DNA damage recognition and signaling were disrupted. Ataxia Telangiectasia Mutated (*ATM*) kinase and Radiation Sensitive 50 (*RAD50*), which are involved in the initial response to double-strand breaks (*DSBs*), were downregulated in stamens, potentially weakening the initiation and propagation of DNA damage signals. Key complexes and regulatory factors involved in end processing, including Topoisomerase II Binding Protein 1 (*TOPBP1*), BRCA1 Interacting Protein C-terminal Helicase 1 (*BRIP1*), and BRCA1-Associated RING Domain protein 1 (*BARD1*), were also significantly downregulated. Members of the RPA protein family, which stabilize single-stranded DNA, exhibited consistent downregulation, directly affecting the formation of nucleoprotein filaments. Furthermore, Radiation Sensitive 54 (*RAD54*) family genes and DNA polymerase δ (*pol δ*) complexes, which are responsible for new strand synthesis, were markedly downregulated, indicating a substantial reduction in repair efficiency using sister chromatids as templates. Critical factors involved in strand displacement and repair via synthesis dependent strand annealing (*SDSA*) or break-induced replication (*BIR*), such as Bloom Syndrome RecQ Like Helicase (*BLM*), were also downregulated. Collectively, these alterations likely impair efficient DNA repair and ligation, thereby contributing to genomic instability during stamen development in *A. donax*.

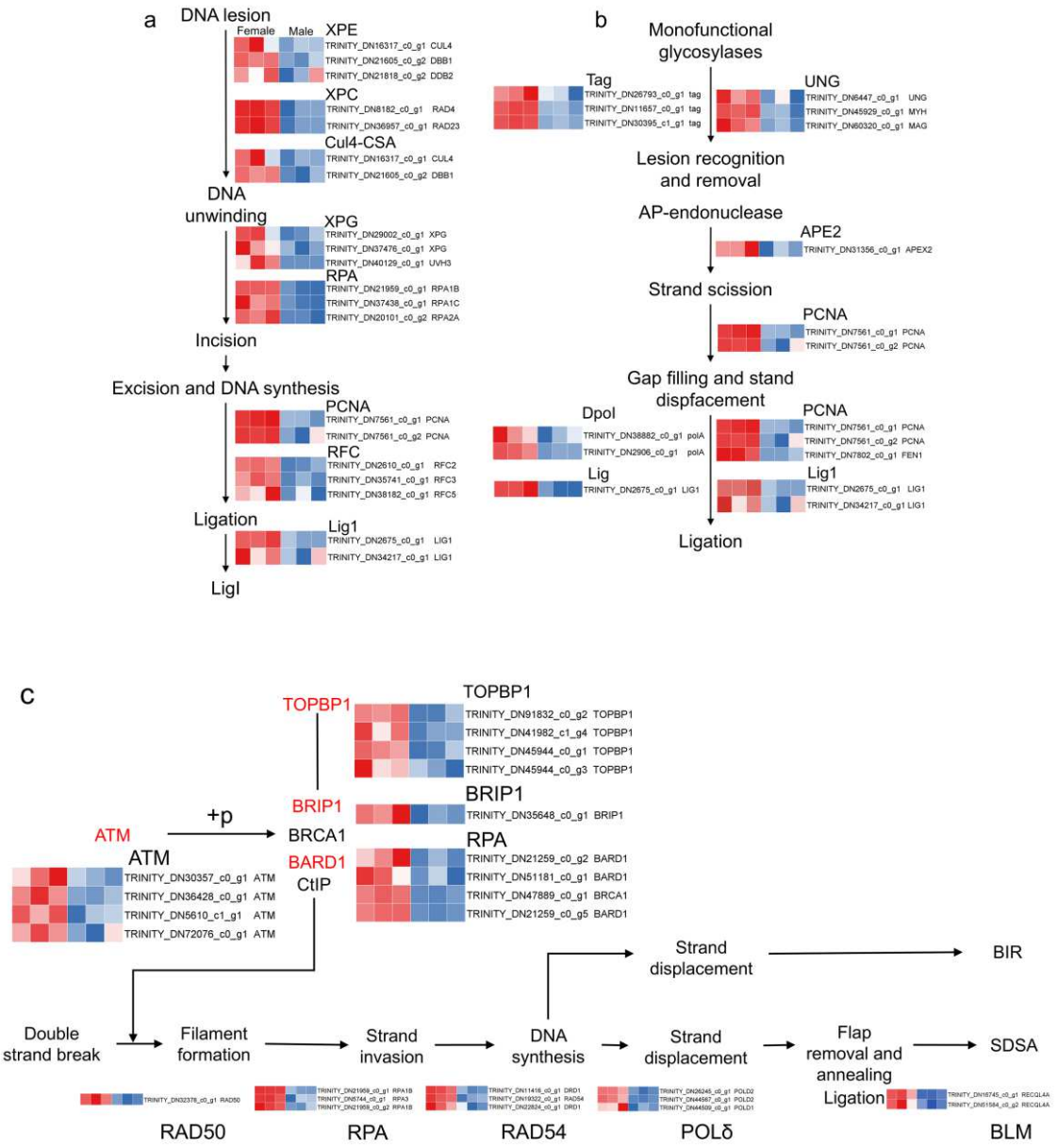

Fig. 8 Expression patterns of DEGs involved in DNA repair pathways (NER, BER, and HR). **a** Expression profiles of DEGs involved in the NER pathway. **b** Expression profiles of DEGs involved in the BER pathway. **c** Expression profiles of DEGs involved in the HR repair pathway. The heat maps indicated relative expression levels of the genes Analysis of downregulated DEGs involved in DNA damage repair pathways. XPE, Xeroderma Pigmentosum complementation group E; XPC, Xeroderma Pigmentosum complementation group C; Cul4-CSA, Cullin 4-Cockayne Syndrome A; XPG, Xeroderma Pigmentosum complementation group G; RPA, Replication Protein A; PCNA, Proliferating Cell Nuclear Antigen; RFC, Replication Factor C; Lig1, DNA Ligase 1; Tag, 3-Methyladenine DNA Glycosylase I; UNG, Uracil-DNA Glycosylase; APE2, Apurinic/Apyrimidinic Endonuclease 2; Dpol, DNA Polymerase I; Lig, DNA Ligase; ATM, Ataxia Telangiectasia Mutated; BRCA1, Breast Cancer susceptibility gene 1; BARD1, BRCA1-Associated RING Domain protein 1; CtIP, CtBP-Interacting Protein; TOPBP1, Topoisomerase II Binding Protein 1, BRIP1; BRCA1 Interacting Protein C-terminal Helicase 1; RPA, Replication Protein A; RAD50, Radiation Sensitive 50; RAD54, Radiation Sensitive 54; POLδ, DNA Polymerase delta; BLM, Bloom Syndrome RecQ Like Helicase; BIR, Break-Induced Replication; SDSA, Synthesis-

Dependent Strand Annealing. +p, phosphorylation

Validation of Expression Profiling by Real-Time Quantitative PCR (RT-qPCR)

To validate the accuracy of the transcriptome sequencing results, a total of nine DEGs (TRINITY_DN10775_c0_g1, TRINITY_DN11897_c0_g1, TRINITY_DN12227_c0_g1, TRINITY_DN11906_c0_g1, TRINITY_DN14555_c0_g1, TRINITY_DN14578_c0_g1, TRINITY_DN15005_c0_g1, TRINITY_DN15887_c0_g1, and TRINITY_DN12740_c0_g1) were randomly selected. The expression profiles of these genes in stamens, pistils, and leaves were examined to determine their consistency with the RNA-seq data. As shown in Fig 9, the expression patterns of all nine genes were largely consistent with the FPKM-based expression profiles obtained from the transcriptome analysis, thereby confirming the reliability of the RNA-seq results.

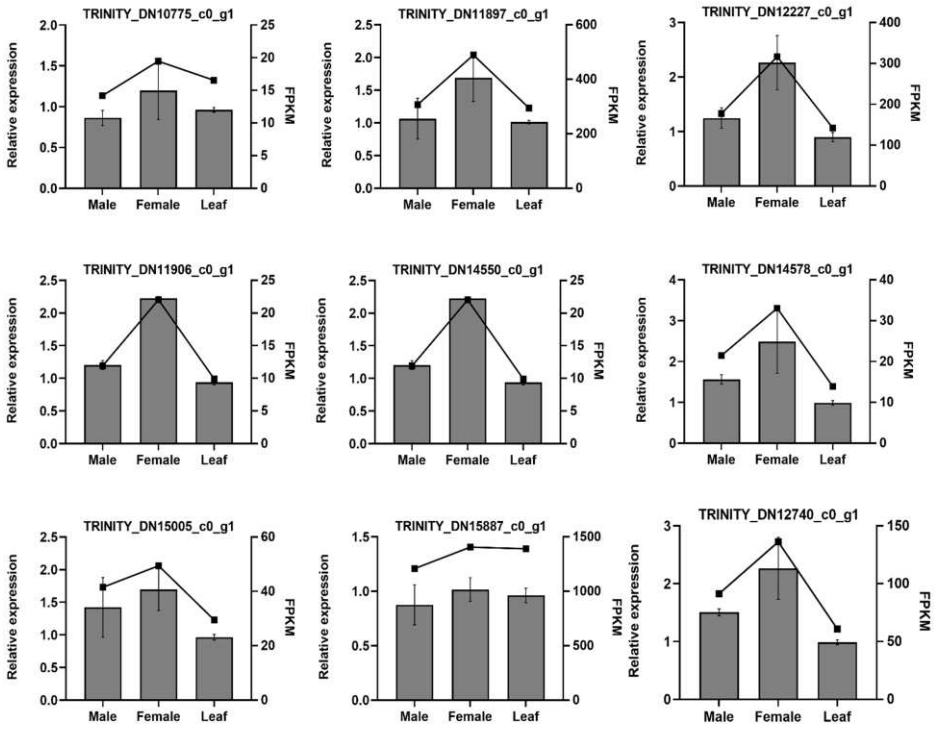

Fig. 9 RT-qPCR analysis of nine randomly selected genes. RT-qPCR results are shown by grey columns, and RNA-Seq findings are represented by lines

Discussion

Tapetum structural abnormalities cause pollen abortion in *A. donax*

The abnormal development of male reproductive organs and anther abortion in *A. donax* (Danelli et al. 2020) constitute major constraints on its sexual reproductive capacity and the efficiency of genetic improvement. Previous studies have demonstrated that the formation and development of the male gametophyte are regulated by a finely coordinated and multilayered regulatory network (Ma 2005). This network encompasses several critical processes, including the maintenance of tapetal cell function, chromosomal stability during meiosis of pollen mother cells, the integrity of microspore exine formation, and the structural organization and metabolic accumulation during pollen maturation (Xu et al. 2014). As one of the most metabolically active tissues in the anther, the tapetum not only supplies essential nutrients and precursor molecules for microspore development but also plays pivotal roles in regulating osmotic balance, redox homeostasis, and signal transduction within the anther

locule (Moreira et al. 2025). Its developmental progression exhibits strict spatiotemporal regulation. Any disruption to its normal development, such as premature degeneration, disordered cellular organization, or loss of structural integrity can directly interfere with the proper progression of microspore development (Hua et al. 2023).

In this study, paraffin sectioning combined with cytological observations revealed pronounced abnormalities in the tapetum of *A. donax* during the early meiotic stage. These abnormalities were characterized by disorganized cellular organization, premature degeneration of certain tapetal cells accompanied by their intrusion into the anther locule, and weakened or locally disrupted connections between the tapetum and the middle layer. Such structural aberrations markedly impair the tapetum's capacity to provide nutritional and metabolic support to developing microspores, thereby adversely affecting the proper deposition of pollen wall precursors. These observations are consistent with previously reported mechanisms of pollen abortion in various angiosperms, in which aberrant tapetal development ultimately leads to microspore abortion. Collectively, these findings suggest that tapetal dysfunction may be a key factor contributing to pollen abortion in *A. donax*.

Meiotic disruption and pollen wall defects lead to pollen abortion in *A. donax*

During male gametogenesis, abnormalities in the meiotic process represent another critical factor underlying pollen abortion (Yang et al. 2021). Extensive studies have demonstrated that aberrant chromosomal behaviors during meiosis, such as lagging chromosomes, chromosome bridge formation (Wang et al. 2024), defective spindle assembly, and irregular cytokinesis can directly lead to unequal nuclear segregation and structural defects in gametophytic cells, thereby giving rise to malformed or functionally impaired pollen grains (Chang et al. 2025). The results of this study indicate that pollen mother cells in *A. donax* exhibit multiple abnormal phenotypes during both meiosis I and meiosis II, including a high frequency of lagging chromosomes, chromosome bridge formation, defective spindle assembly, and incomplete or asymmetric cytokinesis. Furthermore, at the microspore tetrad stage, additional abnormalities were observed, including disorganized arrangement, a reduced number of tetrads, and uneven distribution of cytoplasmic contents. These findings suggest that the mechanical balance governing chromosome segregation is disrupted and that cytokinesis is improperly regulated, ultimately impeding normal microspore formation and providing a cytological basis for subsequent pollen abortion.

During pollen maturation and exine formation, the structural integrity of the pollen wall and the sufficient accumulation of intracellular nutrients are essential for maintaining pollen viability (Liu et al. 2021). Previous studies have demonstrated that the microspore exine consists of a complex sporopollenin matrix (Grienenberger and Quilichini 2021), the deposition of which relies on the coordinated regulation of lipidic and phenolic precursors supplied by the tapetum, along with associated enzymatic systems (An et al. 2025). Disruption of exine formation can result in reduced mechanical strength, decreased stress tolerance, and severely impaired pollen germination capacity (Chen et al. 2017). In this study, pollen grains of *A. donax* frequently exhibited structural abnormalities, including shrinkage, size heterogeneity, invaginated germinal apertures, and abnormal thickening of the exine surrounding the apertures. In addition, a substantial reduction in cytoplasmic content and even vacuolization were observed. In vitro germination assays further showed that the pollen germination rate was only 1.66%, with most pollen tubes being short, curved, or exhibiting arrested growth, indicating extremely low physiological activity. Staining analyses showed that aborted pollen types, including typical abortion, spherical abortion, and stained abortion—were predominant, whereas the proportion of normal pollen was only 8.12%. This distribution suggests that pollen abortion in *A. donax* represents a continuous spectrum of variation rather than being dominated by a single discrete type.

Defects in male reproductive function are further manifested as barriers to successful fertilization. Previous studies have demonstrated that even when pollen production is sufficient, structural abnormalities or reduced physiological activity of pollen grains can hinder the completion of key processes on the stigma surface, including hydration, germination, and pollen tube elongation (Zhang et al. 2022; Lan et al. 2023; Kim et al. 2025). In the

present study, only a limited number of pollen grains were observed adhering to the stigma surface of *A. donax*, and no evidence of pollen tube penetration through the style into the ovary was detected. Ultrastructural observations further revealed pronounced defects in the pollen exine, including aperture invagination, uneven thickening of the exine layers, and leakage of cytoplasmic contents. These abnormalities are unfavorable for pollen adhesion, hydration, and polarized growth on the stigma. Moreover, under both in vivo and in vitro conditions, pollen grains exhibited low germination rates and restricted pollen tube elongation, further confirming severe impairment of male reproductive function. Therefore, the low seed-setting rate in *A. donax* is attributable not only to structural defects arising during pollen development but also to disruption of the fertilization process.

Taken together with cytological observations and previous studies, anther abortion in *A. donax* can be regarded as a complex, multifactorial, and multistage process (Balogh et al. 2012). Abnormal tapetal development disrupts the nutrient supply system, aberrant chromosomal behavior during meiosis, together with defective cytokinesis, impairs microspore formation, abnormal exine deposition and insufficient intracellular accumulation markedly reduce pollen viability and ultimately, limited pollen germination and restricted pollen tube growth result in fertilization failure (Vasupalli et al. 2025). This process is highly consistent, at both cytological and physiological levels, with the canonical mechanisms of pollen abortion reported in Poaceae and other angiosperms, thereby further advancing a systematic understanding of pollen abortion in *A. donax* (Bohra et al. 2025).

In recent years, the role of the ubiquitination system in plant male reproductive development has received increasing attention (Orr et al. 2021). It has been reported that the ubiquitin-proteasome system participates in tapetum development and meiotic progression by mediating the degradation of key transcription factors and cell cycle regulators (Lian et al. 2021). Our results revealed a global upregulation of ubiquitination-related genes in *A. donax* stamens, indicating that enhanced protein degradation may result in the aberrant turnover of critical developmental regulators.

ET and JA signaling pathways regulate pollen abortion in *A. donax*

ET and JA are known to act synergistically during anther development, regulating key processes such as tapetal degeneration and pollen release (Huang et al. 2023). In this study, the ET signaling pathway was consistently upregulated from receptors to downstream EIN3/ERF transcription factors. Concurrently, activation of the JA signaling cascade, including the JAR1-COI1-JAZ-MYC2 module, was also observed. These findings are consistent with previous reports in thermosensitive male-sterile rice lines, in which excessive activation of JA signaling disrupts the timing of tapetal PCD (Fang et al. 2024). The concurrent upregulation of both ET and JA pathways suggests a potential synergistic effect, whereby enhanced hormonal signaling collectively exacerbates pollen abortion in *A. donax*.

Meiotic DNA repair defects lead to pollen abortion in *A. donax*

Regarding cell cycle regulation and DNA repair, previous studies have established that proper cell cycle progression and efficient DNA damage repair during meiosis are essential for the successful completion of pollen mother cell division (Zhang et al. 2023). In this study, downregulated genes were significantly enriched in functions associated with microtubule dynamics, the mitotic cell cycle, and DNA binding, indicating a marked reduction in cellular proliferative capacity and a tendency toward cell cycle arrest or premature terminal differentiation in stamens. Furthermore, the coordinated downregulation of key components involved in NER, BER, and HR pathways suggests that stamens are unable to effectively repair endogenous or ROS-induced DNA damage. This deficiency directly compromises meiotic progression and may lead to the failure of pollen mother cell development. These observations are highly consistent with findings in multiple plant male sterile systems, in which defects in DNA repair result in meiotic abnormalities, indicating that impaired DNA repair capacity is likely a direct cause of pollen abortion (Kurzbauer et al. 2021).

In summary, pollen abortion in *A. donax* is driven by the concerted effects of multi-layered abnormalities.

Premature degeneration of the tapetum and disruption of anther wall structure create an imbalanced microenvironment for microspore development, aberrant chromosomal behavior during meiosis, together with impaired spindle function, directly hinders microspore formation; downregulation of DNA repair pathways compromises the maintenance of genomic stability during cell division; and excessive activation of ET and JA signaling, along with dysregulation of the ubiquitin-proteasome system, further perturbs stamen cell fate and tissue functionality. Collectively, these factors give rise to the characteristic features of pollen abortion in *A. donax*, including reduced pollen number, structural deformities, low viability, and impaired germination capacity. This study not only elucidates the cytological basis of pollen abortion in *A. donax* but also delineates the key molecular regulatory networks, thereby providing a critical theoretical foundation for further investigation of pollen abortion mechanisms and the genetic improvement of perennial grasses.

Supplementary Information

Supplementary Table: Table1 The Sequences of primer for qRT-PCR validate analysis.

Acknowledgments

This work was supported by the Key Research and Development Project of Henan Province（No. 261111111900), Zhengzhou Collaborative Innovation Project of Zhengzhou University (No. 2024XTCX002), Henan Province Major Science and Technology Special Project (No. 231100320100) and Henan Province Science and Technology Research Project (No. 242102111151).

Author contributions

Ruihao Liu: Conceptualization, Data curation, Formal analysis, Visualization, and Writing-original draft. Yixin Huangfu and Beibei Zhang: Conceptualization, Investigation, and Data curation. Xinyu Tan: Investigation and Data curation. Mengxin Huang, Yong Liang and Mingchen Yu: Methodology, Software, and Supervision. Jialin Guo and Zhengqing Xie: Funding acquisition, Methodology, and Data curation. Baoming Tian: Resources and Funding acquisition. Gongyao Shi: Conceptualization, Project administration, Resources, and Supervision. Fang Wei: Conceptualization, Funding acquisition, Project administration, Validation, Writing-review and editing.

Data availability

For inquiries regarding the availability of data, please contact the authors directly.

Declarations

Conflict of interest The authors declare that they have no known competing financial interests or personal relationships that could have appeared to influence the work reported in this paper.

References

An X, Fang C, Zhang S, et al (2025) ZmMS1-orchestrated feedback repression loop regulates ZmACSN2/3—PKSB—TKPR1-1/-2 complex to ensure maize pollen development. Science Bulletin 70:2421–2425. https://doi.org/10.1016/j.scib.2025.03.059

Balogh E, Herr JM, Czakó M, Márton L (2012) Defective development of male and female gametophytes in *Arundo donax* L. (POACEAE). Biomass and Bioenergy 45:265–269. https://doi.org/10.1016/j.biombioe.2012.06.010

Bohra A, Tiwari A, Pareek S, et al (2025) Past and future of cytoplasmic male sterility and heterosis breeding in crop plants. Plant Cell Rep 44:33. https://doi.org/10.1007/s00299-024-03414-5

Chang Y, Chen Z, Chen W, et al (2025) KNUCKLES promotes meiotic cell-cycle progression by directly repressing the expression of KRP1 and KRP3 to ensure male fertility. Plant Commun 7:101610. https://doi.org/10.1016/j.xplc.2025.101610

Chen X, Zhang H, Sun H, et al (2017) IRREGULAR POLLEN EXINE1 Is a Novel Factor in Anther Cuticle and

Pollen Exine Formation1[OPEN]. Plant Physiol 173:307–325. https://doi.org/10.1104/pp.16.00629

Chen Y, Liu C, Zhang X, et al (2025) A Novel Laboratory Protocol for Pollen Viability Assessment to Inform Biosafety Evaluation of Transgenic Rice (*Oryza sativa* L.). Agriculture 15:. https://doi.org/10.3390/agriculture15232420

Corno L, Pilu R, Adani F (2014) *Arundo donax* L.: A non-food crop for bioenergy and bio-compound production. Biotechnology Advances 32:1535–1549. https://doi.org/10.1016/j.biotechadv.2014.10.006

Cristaldi A, Oliveri Conti G, Cosentino SL, et al (2020) Phytoremediation potential of *Arundo donax* (Giant Reed) in contaminated soil by heavy metals. Environmental Research 185:109427. https://doi.org/10.1016/j.envres.2020.109427

Danelli T, Laura M, Savona M, et al (2020) Genetic Improvement of *Arundo donax* L.: Opportunities and Challenges. Plants 9:. https://doi.org/10.3390/plants9111584

Fang Y, Guo D, Wang Y, et al (2024) Rice transcriptional repressor OsTIE1 controls anther dehiscence and male sterility by regulating JA biosynthesis. Plant Cell 36:1697–1717. https://doi.org/10.1093/plcell/koae028

Gómez JF, Talle B, Wilson ZA (2015) Anther and pollen development: A conserved developmental pathway. J Integr Plant Biol 57:876–891. https://doi.org/10.1111/jipb.12425

Grienenberger E, Quilichini TD (2021) The Toughest Material in the Plant Kingdom: An Update on Sporopollenin. Front Plant Sci 12:703864. https://doi.org/10.3389/fpls.2021.703864

Haddadchi A, Gross CL, Fatemi M (2013) The expansion of sterile *Arundo donax* (Poaceae) in southeastern Australia is accompanied by genotypic variation. Aquatic Botany 104:153–161. https://doi.org/10.1016/j.aquabot.2012.07.006

Hardion L, Verlaque R, Rosato M, et al (2015) Impact of polyploidy on fertility variation of Mediterranean *Arundo* L. (Poaceae). Comptes Rendus Biologies 338:298–306. https://doi.org/10.1016/j.crvi.2015.03.013

Hua M, Yin W, Fernández Gómez J, et al (2023) Barley TAPETAL DEVELOPMENT and FUNCTION1 (HvTDF1) gene reveals conserved and unique roles in controlling anther tapetum development in dicot and monocot plants. New Phytologist 240:173–190. https://doi.org/10.1111/nph.19161

Huang H, Chen Y, Wang S, et al (2023) Jasmonate action and crosstalk in flower development and fertility. J Exp Bot 74:1186–1197. https://doi.org/10.1093/jxb/erac251

Kim E-J, Son Y, Kim J-H, et al (2025) OsPRK1/2/3-mediated reactive oxygen species signaling is required for pollen tube germination in rice. Journal of Integrative Plant Biology 67:1965–1981. https://doi.org/10.1111/jipb.13921

Kurzbauer M-T, Janisiw MP, Paulin LF, et al (2021) ATM controls meiotic DNA double-strand break formation and recombination and affects synaptonemal complex organization in plants. Plant Cell 33:1633–1656. https://doi.org/10.1093/plcell/koab045

Lan Z, Song Z, Wang Z, et al (2023) Antagonistic RALF peptides control an intergeneric hybridization barrier on

Brassicaceae stigmas. Cell 186:4773-4787.e12. https://doi.org/10.1016/j.cell.2023.09.003

Li B, Dewey CN (2011) RSEM: accurate transcript quantification from RNA-Seq data with or without a reference genome. BMC Bioinformatics 12:323. https://doi.org/10.1186/1471-2105-12-323

Lian J-P, Yang Y-W, He R-R, et al (2021) Ubiquitin-dependent Argonauteprotein MEL1 degradation is essential for rice sporogenesis and phasiRNA target regulation. Plant Cell 33:2685–2700. https://doi.org/10.1093/plcell/koab138

Lino G, Espigul P, Nogués S, Serrat X (2023) *Arundo donax* L. growth potential under different abiotic stress. Heliyon 9:e15521. https://doi.org/10.1016/j.heliyon.2023.e15521

Liu S, Li Z, Wu S, Wan X (2021) The essential roles of sugar metabolism for pollen development and male fertility in plants. The Crop Journal 9:1223–1236. https://doi.org/10.1016/j.cj.2021.08.003

Lou Y, Zhou H-S, Han Y, et al (2018) Positive regulation of AMS by TDF1 and the formation of a TDF1–AMS complex are required for anther development in *Arabidopsis thaliana*. New Phytologist 217:378–391. https://doi.org/10.1111/nph.14790

Ma H (2005) MOLECULAR GENETIC ANALYSES OF MICROSPOROGENESIS AND MICROGAMETOGENESIS IN FLOWERING PLANTS. Annu Rev Plant Biol 56:393–434. https://doi.org/10.1146/annurev.arplant.55.031903.141717

Moon S, Hong W-J, Kim Y-J, et al (2020) Comparative Transcriptome Analysis Reveals Gene Regulatory Mechanism of UDT1 on Anther Development. J Plant Biol 63:289–296. https://doi.org/10.1007/s12374-020-09250-w

Moreira GLLS, Ferreira MEP, Linhares FS (2025) Identity Transitions of Tapetum Phases: Insights into Vesicular Dynamics and in Mortem Support During Pollen Maturation. Plants 14:. https://doi.org/10.3390/plants14050749

Nikhade CA, Makde KH (2014) REPRODUCTIVE BEHAVIOR OF *ARUNDO DONAX* L.

Orr JN, Waugh R, Colas I (2021) Ubiquitination in Plant Meiosis: Recent Advances and High Throughput Methods. Front Plant Sci 12:. https://doi.org/10.3389/fpls.2021.667314

Peterson R, Slovin JP, Chen C (2010) A Simplified Method for Differential Staining of Aborted and Non-Aborted Pollen Grains. IJPB 1:e13. https://doi.org/10.4081/pb.2010.e13

Roberto Pilu (2012) Giant reed *(Arundo donax* L.): A weed plant or a promising energy crop? Afr J Biotechnol 11:. https://doi.org/10.5897/AJB11.4182

Sánchez E, Lino G, Serrat X, Nogués S (2021) Characterization of Different *Arundo donax* L. Clones from the Mediterranean Region. Agronomy 11:. https://doi.org/10.3390/agronomy11071347

Tidy AC, Ferjentsikova I, Vizcay-Barrena G, et al (2022) Sporophytic control of pollen meiotic progression is mediated by tapetum expression of *ABORTED MICROSPORES*. Journal of Experimental Botany 73:5543–5558. https://doi.org/10.1093/jxb/erac225

Vasupalli N, Mogilicherla K, Shaik V, et al (2025) Advances in plant male sterility for hybrid seed production: an overview of conditional nuclear male sterile lines and biotechnology-based male sterile systems. Front Plant Sci 16:. https://doi.org/10.3389/fpls.2025.1540693

Wang B, Liang N, Shen X, et al (2024) Cytological and transcriptomic analyses provide insights into the pollen fertility of synthetic allodiploid *Brassica juncea* hybrids. Plant Cell Rep 43:23. https://doi.org/10.1007/s00299-023-03089-4

Wang N, Li X, Zhu J, Yang Z-N (2025) Molecular and cellular mechanisms of photoperiod- and thermo-sensitive genic male sterility in plants. Molecular Plant 18:26–41. https://doi.org/10.1016/j.molp.2024.12.012

Wei S, Ma L (2023) Comprehensive Insight into Tapetum-Mediated Pollen Development in *Arabidopsis thaliana.* Cells 12:247. https://doi.org/10.3390/cells12020247

Xu J, Ding Z, Vizcay-Barrena G, et al (2014) ABORTED MICROSPORES Acts as a Master Regulator of Pollen Wall Formation in *Arabidopsis*. Plant Cell 26:1544–1556. https://doi.org/10.1105/tpc.114.122986

Yang C, Song J, Ferguson AC, et al (2017) Transcription Factor MYB26 Is Key to Spatial Specificity in Anther Secondary Thickening Formation1[CC-BY]. Plant Physiol 175:333–350. https://doi.org/10.1104/pp.17.00719

Yang F, Fernández-Jiménez N, Tučková M, et al (2021) Defects in meiotic chromosome segregation lead to unreduced male gametes in *Arabidopsis* SMC5/6 complex mutants. Plant Cell 33:3104–3119. https://doi.org/10.1093/plcell/koab178

Zhang D, Jiang Q, Liang D, et al (2021) The Potential Application of Giant Reed (*Arundo donax*) in Ecological Remediation. Front Environ Sci 9:. https://doi.org/10.3389/fenvs.2021.652367

Zhang F, Shi W, Zhou Y, et al (2023) RAD51C-RAD51D interplays with MSH5 and regulates crossover maturation in rice meiosis. New Phytologist 239:1790–1803. https://doi.org/10.1111/nph.19095

Zhang L, Liu Y, Wei G, et al (2022) POLLEN WALL ABORTION 1 is essential for pollen wall development in rice. Plant Physiol 190:2229–2245. https://doi.org/10.1093/plphys/kiac435

Zhou L, Mao Y-C, Yang Y-M, et al (2024) Temperature and light reverse the fertility of rice P/TGMS line ostms19 via reactive oxygen species homeostasis. Plant Biotechnology Journal 22:2020–2032. https://doi.org/10.1111/pbi.14322

Supplementary Files

This is a list of supplementary files associated with this preprint. Click to download.

- Table.docx
- SupplementaryMaterial.docx